

# Measurement of the Interfacial Tension between Coexisting Isotropic and Nematic Phases of a Lyotropic Polymer Liquid Crystal

Wei-liang Chen, Takahiro Sato,\* and Akio Teramoto

Department of Macromolecular Science, Osaka University, Toyonaka, Osaka 560, Japan

Received December 12, 1995; Revised Manuscript Received March 18, 1996<sup>®</sup>

**ABSTRACT:** The interfacial tension and molecular alignment were studied for the interface between coexisting isotropic and nematic phases of a toluene solution of poly(*n*-hexyl isocyanate). A polarizing microscopic observation revealed that the nematic phase in the vicinity of the interface is aligned homogeneously, i.e., the director is parallel to the interface, consistent with the prediction of Doi and Kuzuu for rodlike polymer solutions. The value of the interfacial tension is 0.024 dyn/cm, as compared with the theoretical value (=0.011 dyn/cm).

## 1. Introduction

Macro- and microphase separations in polymeric systems produce an interface whose thickness is comparable to the dimension of polymer chains. Polymer chains in the interfacial region are subjected to an inhomogeneous molecular field, and they should differ from polymer chains in the bulk with respect to their conformation, intermolecular interaction, and alignment.<sup>1</sup> These differences yield the interfacial tension  $\gamma$ , which contains information of the state of the polymer chain in the interfacial region.

Interfacial tensions for phase-separated systems of flexible polymer solutions and blends were measured by several workers,<sup>2–6</sup> and the corresponding theories<sup>1</sup> have been formulated on various theoretical bases (scaling law, van der Waals type theory, etc.). For liquid crystalline polymers, Doi and Kuzuu<sup>7</sup> theoretically calculated  $\gamma$  between coexisting isotropic and nematic phases of rodlike polymer solutions on the basis of Onsager's theory<sup>8,9</sup> with the second virial approximation. However, they had no experimental data to compare with their result. To our best knowledge, no attempt has ever been reported to measure  $\gamma$  for lyotropic polymer liquid crystal systems to test the Doi–Kuzuu prediction.

In the present study, we measured the interfacial tension between coexisting isotropic and nematic phases of a toluene solution of poly(*n*-hexyl isocyanate) (PHIC), a molecularly well-characterized semiflexible polymer,<sup>10–13</sup> and compared it with the theory of Doi and Kuzuu. We chose this system since it is regarded as a standard system of lyotropic polymer liquid crystals amenable to a quantitative analysis. Indeed, its bulk properties such as osmotic pressure,<sup>14</sup> isotropic–nematic phase diagrams,<sup>15–17</sup> and orientational order parameter<sup>18,19</sup> as well as dilute solution properties have been studied in detail and compared favorably with relevant theories.

## 2. Experimental Section

**Preparation of Phase-Separated Solutions.** A PHIC sample was fractionated by an established method,<sup>12,13</sup> and one selected fraction was used for the following measurements. The weight-average molecular weight  $M_w$  of the fraction was determined as  $6.24 \times 10^4$  by light scattering, and the polydis-

persity  $M_w/M_n$  was found to be 1.06 by GPC. Toluene used as solvent was fractionally distilled using sodium as desiccant.

A biphasic toluene solution of the PHIC fraction was prepared by mixing weighed amounts of the fraction and toluene in a test tube with a stopper and stirring the mixture by a magnetic chip for 1–2 days in an air bath thermostated at 25 °C. This biphasic solution was centrifuged at 4000 rpm at 25 °C in a Sorval RC centrifuge to achieve complete phase separation. After centrifugation, the test tube was transferred to a water bath thermostated at 25 °C, and the isotropic and nematic phases were carefully sucked into syringes to be used for measurements of the interfacial tension as well as the binodal concentrations described below.

**Pendant-Drop Experiment.** The interfacial tension between the coexisting isotropic and nematic phases was measured by the pendant-drop method.<sup>20,21</sup> The coexisting isotropic phase sucked into a syringe was transferred into a rectangular cuvette with a 10-mm width, while a microsyringe containing the coexisting nematic phase was set on the top of the cuvette. Evaporation of the solvent was prevented by a Teflon cap and Teflon seal. The temperature of the isotropic and nematic solutions was thermostated at 25 °C. A small amount of the nematic solution was pushed out of the microsyringe to form a pendant drop into the isotropic phase. A picture of the pendant drop was taken under crossed polar conditions by a camera horizontally mounted on a traveling stage. The magnification of the pictures was determined by a microscopic ruler photographed by the same camera.

A meridian curve of the pendant drop was expressed in terms of the  $xy$  coordinates. Here, the  $x$  and  $y$  axes coincide with the tangent and normal lines at the apex of the drop, respectively. About 200 sets of the  $xy$  coordinates of the meridian curve were taken from the picture (the negative film) of the pendant drop by using a projector (Nikon, Shadow Graph Model 6) with a magnification of 20. The  $xy$  coordinate sets measured were numbered as  $-n, -(n-1), \dots, 0, \dots, (n-1), n$ . The zeroth set was chosen to be the coordinates of the apex of the drop, i.e., the origin of the  $xy$  coordinates  $[(x_0, y_0) = (0, 0)]$ , and the measurements were made so that the  $y$  coordinates of the  $-i$ th and  $i$ th sets were equal to each other.

The  $y$  axis on the projector was made to coincide with the vertical direction of the pendant drop in the film by tilting the film so that the quantity  $(x_i + x_{-i})/2$  should be independent of  $i$  ( $i = 1, 2, \dots, n$ ). On the other hand, the origin of the  $x$  axis on the projector was determined so that the mean value  $\delta \equiv n^{-1} \sum_{i=1}^n \frac{1}{2}(x_i + x_{-i})$  was equal to zero. [Actually, after provisional values of  $x_{\pm i}$  ( $1 \leq i \leq n$ ) were determined, the final values of  $x_{\pm i}$  were redefined by subtracting  $\delta$  from the provisional  $x_{\pm i}$ .]

**Binodal Concentrations.** The polymer weight fractions in the coexisting isotropic ( $w_i$ ) and nematic ( $w_n$ ) solutions were determined gravimetrically to be 0.2274 and 0.2471, respectively. These values are consistent with the previous measurements.<sup>16</sup>

<sup>®</sup> Abstract published in *Advance ACS Abstracts*, May 1, 1996.

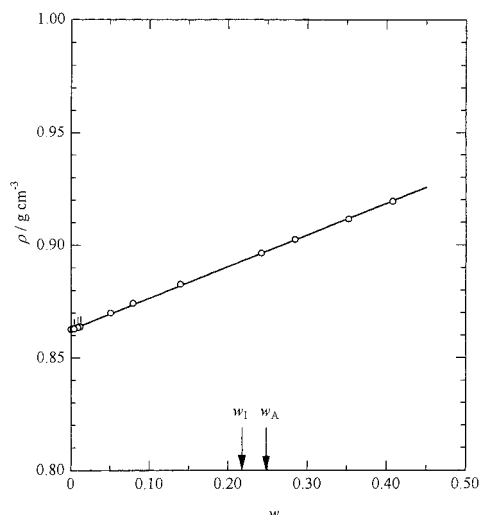


**Figure 1.** Density of the PHIC–toluene system as a function of the PHIC weight fraction  $w$  (25 °C); data points with pips, taken from ref 16.

**Density Measurement.** The density  $\rho$  of the PHIC–toluene system was measured by a Lipkin–Devoson type pycnometer of 5 cm<sup>3</sup> capacity over the polymer concentration ranging from the isotropic to the nematic region. Figure 1 shows the results. The data points follow a straight line, with no inflection at the phase boundary concentrations. The densities  $\rho_I$  of the isotropic phase and  $\rho_A$  of the nematic phase were estimated from the straight line;  $\rho_I = 0.8945$  g/cm<sup>3</sup> and  $\rho_A = 0.8972$  g/cm<sup>3</sup>. From these densities, the polymer mass concentrations  $c_I$  and  $c_A$  of the coexisting isotropic and nematic phases were calculated to be 0.2034 and 0.2217 g/cm<sup>3</sup>, respectively.

**Polarizing Microscopic Observation of the Interface.** A biphasic PHIC solution was placed into a drum-shaped cell with a 10-mm diameter and 2-mm thickness and centrifuged at 2000 rpm for 2 h to achieve complete phase separation. The interfacial region in the cell was observed by a polarizing microscope (Olympus BHS-P) under crossed polar conditions. The extinction for the nematic phase in the vicinity of the interface was observed when the interfacial line was oriented parallel to the crossed polars. Thus the director of the nematic phase near the interface should be oriented parallel or normal to the interface.

The interfacial region was also observed by inserting a compensator with the retardation of 530 nm oriented at 45° to the direction of the crossed polarizers. When the interfacial line was parallel to the azimuth of vibration of the fast ray in the compensator, a subtraction color was observed at the nematic phase near the interface. This indicates that the refractive index of the nematic phase parallel to the interface is larger than that normal to the interface.<sup>22</sup>

### 3. Results and Discussion

An example of a meridian curve measured for a pendant drop of the nematic phase formed in the coexisting isotropic phase is shown in Figure 2; its  $xy$  coordinates are represented by filled circles. The size of this pendant drop is close to the size of the critical drop which remains suspended at the top of the microsyringe. The unfilled circles in Figure 2 show the locus of  $y_i$  vs  $(x_i + x_{-i})/2$  ( $1 \leq i \leq n$ ; cf. Experimental Section) constructed from the experimental  $xy$  coordinate sets. As mentioned in the Experimental Section, the constancy of  $(x_i + x_{-i})/2$  guaranteed that the  $y$  axis coincides with the vertical direction of the pendant drop. Since the  $x$  axis coincides with the normal to the meridian curve at the apex, the absolute values of  $x_i$

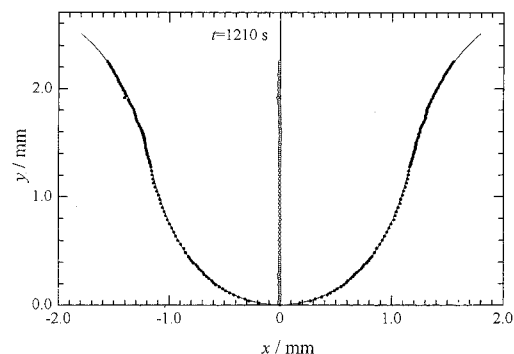


**Figure 2.** Meridian curve for a pendant drop of the nematic phase formed in the coexisting isotropic phase; filled circles, experimental data; curve, theoretical result obtained by least squares regression; unfilled circles, plot of  $y_i$  vs  $(x_i + x_{-i})/2$ .

and  $x_{-i}$  should be equal. The relative difference of  $x_i$  (or  $|x_{-i}|$ ) from their mean value

$$\bar{x}_i \equiv \frac{1}{2}(x_i + |x_{-i}|)$$

was less than 1% except for 3 of 98 data sets, which demonstrates that the measurements of  $x_{\pm i}$  were accurate.

The experimental data points of the meridian curve shown in Figure 2 are fitted to the theoretical meridian curve calculated by the Young–Laplace equation<sup>20,21</sup> in the following way. First, the theoretical curve is calculated numerically by the Young–Laplace equation with chosen values of  $r_0$  and  $\beta$ . Here,  $r_0$  is the radius of curvature at the drop apex and  $\beta$  is the dimensionless shape factor of the drop. Then the mean square deviation between theory and experiment

$$\overline{\Delta^2} \equiv \frac{1}{n} \sum_{i=1}^n \{[\bar{x}_i - x_{\text{cal}}(s_i)]^2 + [y_i - y_{\text{cal}}(s_i)]^2\} \quad (1)$$

is calculated.<sup>21</sup> Here  $s_i$  represents the contour point (the contour distance from the drop apex) on the theoretical meridian curve which is closest to the experimental data point  $(\bar{x}_i, y_i)$ , and  $x_{\text{cal}}(s_i)$  and  $y_{\text{cal}}(s_i)$  are the  $x$  and  $y$  coordinates, respectively, of the theoretical contour point  $s_i$ .<sup>23</sup> Values of  $\overline{\Delta^2}$  are calculated for the different sets of  $r_0$  and  $\beta$  to search for the set giving the minimum  $\overline{\Delta^2}$ .

For the  $(\bar{x}_i, y_i)$  data points in Figure 2,  $\overline{\Delta^2}$  takes a definite minimum at  $r_0 = 0.916$  mm and  $\beta = 0.862$ . The solid curve in Figure 2 shows the theoretical meridian curve giving the minimum  $\overline{\Delta^2}$ , which fits the experimental data points (filled circles).

The meridian curve of the pendant drop changed its shape when time  $t$  elapsed after forming the drop from the microsyringe. The meridian curve shown in Figure 2 was that at  $t = 1210$  s. Figure 3 demonstrates the gradual approaches of  $r_0$  and  $\beta$  to equilibrium values. The slow process may result from low translational and rotational mobilities of PHIC chains in the concentrated phases.

The interfacial tension  $\gamma$  can be calculated from<sup>20,21</sup>

$$\gamma = g\Delta\rho r_0^2/\beta \quad (2)$$

where  $g$  is the gravitational acceleration and  $\Delta\rho$  is the density difference between the coexisting two phases. The equilibrium value of  $r_0^2/\beta$  in this equation was

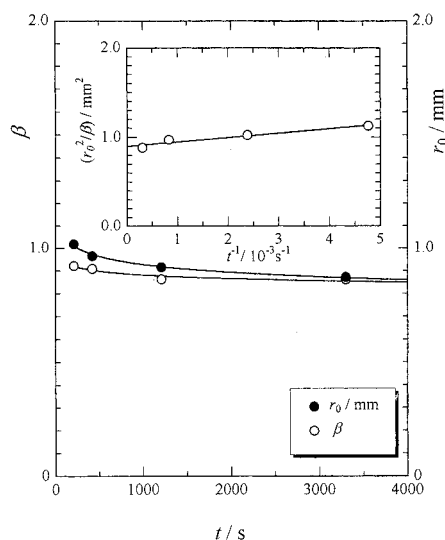


**Figure 3.** Size and shape parameters ( $r_0$  and  $\beta$ ) of the pendant drop plotted against  $t$ ; insert, plot of  $r_0^2/\beta$  vs  $t^{-1}$ .

**Table 1.** Comparison between Experiment and Theory

quantity	experiment	Onsager-type theory	scaled particle theory <sup>c</sup>
$\gamma/(\text{dyn cm}^{-1})$	0.024	0.0109 <sup>a</sup>	
$c_l/(\text{g cm}^{-3})$	0.203	0.0539 <sup>b</sup>	0.182 <sup>c</sup>
$c_A/(\text{g cm}^{-3})$	0.223	0.0724 <sup>b</sup>	0.198 <sup>c</sup>

<sup>a</sup> Reference 7. <sup>b</sup> Reference 8. <sup>c</sup> Reference 28.

obtained by the extrapolation of  $r_0^2/\beta$  to infinite  $t$  (cf. the insert in Figure 3). The  $\gamma$  value of  $2.4 \times 10^{-2}$  dyn/cm for the isotropic–nematic interface of the PHIC–toluene system is of the same order as those of low-molar-mass thermotropic liquid crystals;  $\gamma$  for the isotropic–nematic interface of MBBA was reported to be  $(2.3 \pm 0.4) \times 10^{-2}$  or  $1.6 \times 10^{-2}$  dyn/cm<sup>25</sup> and those of cyanobiphenyls (5CB–8CB) to range from  $0.7 \times 10^{-2}$  to  $1.8 \times 10^{-2}$  dyn/cm.<sup>26</sup>

Doi and Kuzuu<sup>7</sup> calculated  $\gamma$  for solutions of hard rods based on the Onsager-type theory neglecting the third and higher virial terms. Their result is

$$\gamma = 0.257 \frac{k_B T}{dL} (1 + 1.75 \cos^2 \theta)^{1/2} \quad (3)$$

where  $d$  and  $L$  are the hard-core diameter and length of the rodlike polymer, respectively,  $\theta$  is the angle between the director in the nematic phase and the normal to the interface, and  $k_B T$  is the Boltzmann constant multiplied by the absolute temperature. Equation 3 predicts that the homogeneous alignment ( $\theta = \pi/2$ ) in the coexisting nematic phase minimizes the interfacial energy, and thus this alignment should be realized at equilibrium.

As mentioned in the Experimental Section, the polarizing microscopic observation on the nematic phase near the interface showed that the refractive index parallel to the interface was larger than that normal to the interface. Since the PHIC molecule is positively birefringent,<sup>27</sup> this observation indicates that the director near the interface should be parallel to the interface. (A tilted alignment is inconsistent with the position of extinction; see Experimental Section.) This is consistent with the prediction of Doi and Kuzuu.

Table 1 compares the experimental result of  $\gamma$  for the PHIC–toluene system with the Doi–Kuzuu theory with  $\theta = \pi/2$ . The theoretical  $\gamma$  was calculated by using  $L =$

84.3 nm and  $d = 1.15$  nm for the PHIC fraction. The former was calculated from  $M_w$  along with  $M_L$  (the molar mass per unit contour length) =  $740 \text{ nm}^{-1}$ ,<sup>12</sup> while the latter was previously estimated from osmotic pressure data of the PHIC–toluene system.<sup>14</sup> The theory properly predicts the order of  $\gamma$  for the PHIC–toluene system without any adjustable parameters, but the theoretical magnitude of  $\gamma$  is about half the experimental one.

Table 1 also compares the experimental results of  $c_l$  and  $c_A$  with the predictions of the Onsager theory,<sup>8</sup> which has the same theoretical basis as the Doi–Kuzuu theory for  $\gamma$ ; i.e., both use the hard-rod model and the second virial approximation. This theory for the binodal concentrations also underestimates the experimental results. Previous publications<sup>28–30</sup> demonstrate that this disagreement between the Onsager theory and experiment is greatly reduced by use of the scaled particle theory for the wormlike spherocylinder model which considers the effects of the polymer chain flexibility and the higher virial terms (cf. the fourth column of Table 1). This implies that the disagreement between theory and experiment for  $\gamma$  also may be interpreted by the same effects. However, at present, there is no corresponding theory of  $\gamma$  based on the scaled particle theory with the wormlike spherocylinder model.

**Acknowledgment.** This work was financially supported by a Grant-in-Aid for Scientific Research from the Ministry of Education, Science, and Culture of Japan.

## References and Notes

- (1) *Physics of Polymer Surfaces and Interfaces*; Sanchez, I. C., Ed.; Butterworth-Neimann: Boston, 1992.
- (2) Langhammer, G.; Nestler, L. *Makromol. Chem.* **1965**, *88*, 179.
- (3) Wu, S. J. *Macromol. Sci.* **1974**, *C10*, 1.
- (4) Nose, T.; Tan, T. V. *J. Polym. Sci., Polym. Lett. Ed.* **1976**, *14*, 705.
- (5) Shinozaki, K.; Tan, T. V.; Saito, Y.; Nose, T. *Polymer* **1982**, *23*, 728.
- (6) Nose, T. *Macromolecules* **1995**, *28*, 3702.
- (7) Doi, M.; Kuzuu, N. *J. Appl. Polym. Sci., Polym. Symp.* **1985**, *41*, 65.
- (8) Onsager, L. *Ann. N.Y. Acad. Sci.* **1949**, *51*, 627.
- (9) Odijk, T. *Macromolecules* **1986**, *19*, 2313.
- (10) Murakami, H.; Norisuye, T.; Fujita, H. *Macromolecules* **1980**, *13*, 345.
- (11) Kuwata, M.; Murakami, H.; Norisuye, T.; Fujita, H. *Macromolecules* **1984**, *17*, 2731.
- (12) Itou, T.; Chikiri, H.; Teramoto, A.; Aharoni, S. M. *Polym. J.* **1988**, *20*, 143.
- (13) Jinbo, Y.; Sato, T.; Teramoto, A. *Macromolecules* **1994**, *27*, 6080.
- (14) Itou, T.; Sato, T.; Teramoto, A.; Aharoni, S. M. *Polym. J.* **1988**, *20*, 1049.
- (15) Conio, G.; Bianchi, E.; Ciferri, A.; Krigbaum, W. R. *Macromolecules* **1984**, *17*, 856.
- (16) Itou, T.; Teramoto, A. *Macromolecules* **1988**, *21*, 2225.
- (17) Sato, T.; Ikeda, N.; Itou, T.; Teramoto, A. *Polymer* **1989**, *30*, 311.
- (18) Wang, H.; DuPré, D. B. *J. Chem. Phys.* **1992**, *96*, 1523.
- (19) Wang, H.; Wittebort, R. J.; DuPré, D. B. *J. Chem. Phys.* **1993**, *99*, 7449.
- (20) Andreas, J. M.; Hauser, E. A.; Tucker, W. B. *J. Phys. Chem.* **1938**, *42*, 1001.
- (21) Rotenberg, Y.; Boruvka, L.; Neumann, A. W. *J. Colloid Interface Sci.* **1983**, *93*, 169.
- (22) Slayter, E. M.; Slayter, H. S. *Light and Electron Microscopy*; Cambridge University Press: Cambridge, 1992.
- (23) The theoretical contour point  $s_i$  closest to the  $i$ th experimental data point fulfills the condition

$$[\bar{x}_i - x_{\text{cal}}(s_i)] \cos \phi(s_i) + [y_i - y_{\text{cal}}(s_i)] \sin \phi(s_i) = 0$$

where  $\phi(s_i)$  is the angle between the tangent at the point  $s_i$

and the  $x$  axis. We can find the contour point  $s_i$  by this condition to calculate  $\Delta^2$ .

- (24) Langevin, D.; Bouchiat, M. A. *Mol. Cryst. Liq. Cryst.* **1973**, 22, 317.
- (25) Williams, R. *Mol. Cryst. Liq. Cryst.* **1976**, 35, 349.
- (26) Faetti, S.; Palleschi, V. *J. Chem. Phys.* **1984**, 81, 6254.
- (27) Tsvetkov, V. N. *Rigid-Chain Polymers*; Consultants Bureau: New York, 1989. Coles, H. J.; Gupta, A. K.; Marchal,

E. *Macromolecules* **1977**, 10, 182.

- (28) Sato, T.; Teramoto, A. *Mol. Cryst. Liq. Cryst.* **1990**, 178, 143.
- (29) Sato, T.; Teramoto, A. In *Ordering in Macromolecular Systems*; Teramoto, A., Kobayashi, M., Norisuye, T., Eds.; Springer-Verlag: Berlin, Heidelberg, 1994; p 155.
- (30) Sato, T.; Teramoto, A. *Acta Polym.* **1994**, 45, 399.

MA951832Y